

Estimating mineral scaling and porosity alterations during the circulation test at Utah-FORGE site using reactive transport modeling

Ram Kumar^{*1,2}, Mengnan Li¹, Lynn B. Munday¹, Stuart Simmons³, Ghanshyam Neupane^{1,2}, Robert Smith^{2,4}, Rachael Colldeweih^{1,2}, Travis McLing^{1,2}, Robert Podgorney¹

¹Idaho National Laboratory, Idaho Falls, Idaho, U.S.A.

²Center for Advanced Energy Studies, Idaho Falls, Idaho, U.S.A.

³Energy & Geoscience Institute, University of Utah, Salt Lake City, Utah, U.S.A.

⁴Earth and Spatial Sciences, University of Idaho, Moscow, Idaho, U.S.A.

*Ram.kumar@inl.gov

Keywords: FORGE, EGS, THC, Reactive Transport Modeling, DFN, Mineralogical Changes

ABSTRACT

The Utah Frontier Observatory for Research in Geothermal Energy (FORGE) field-scale laboratory was created to promote and expedite the development of Enhanced Geothermal System (EGS) resources. This paper aims to enhance the understanding of the thermal-hydrological-chemical (THC) processes involved with EGS operation at the FORGE site. The primary objective is to evaluate the mineralogical changes and their impact on porosity and flow, using chemical speciation data from injected and produced water collected during the circulation test at the deepest well, located at 9,500 feet. Leveraging reservoir and geochemistry data, a 3-dimensional THC model was created to investigate water-rock interactions and flow in porous and fractured media using the FALCON (Fracturing And Liquid CONvection) code and The Geochemist's Workbench. The model's results forecasted the spatial and temporal distribution of dissolved and precipitated minerals and the net changes in porosity due to reactive geochemistry temperature variations during the circulation test. Mineralogical changes were more significant in the fracture network compared to the rock matrix, owing to the preferential flow associated with higher permeability of fractures. Additionally, calcite precipitation was dominant among the minerals, with mica precipitation also observed along the fractured plane near the injection well. The spatial distribution of precipitated minerals indicated how fluid transport in the wells moves these minerals further along the fractured planes. The model predictions, such as pH and aqueous species, were consistent with the produced water data. The results of this study will aid in the development of EGS resources and suggest mitigation and operational strategies for sustainable geothermal production.

1. INTRODUCTION

The Frontier Observatory for Research in Geothermal Energy (FORGE) is a large-scale lab situated in a remote area of southwest Utah, 16 km northeast of Milford. Established by the US Department of Energy (DOE), Utah FORGE aims to advance technologies for commercializing Enhanced Geothermal Systems (EGS). Unlike conventional geothermal resources that depend on natural permeability, EGS can tap into the Earth's heat in areas with hot dry rock, expanding renewable energy production. Key research at Utah FORGE includes ensuring fluid circulation between wells and accurate geological characterization of the reservoir (Moore et al., 2019). Since 2015, several wells have been drilled at Utah FORGE, including two closely spaced, highly deviated wells for circulation testing. The injection well, 16A(78)-32, was completed in January 2021, and the production well, 16B(78)-32, was completed in June 2023. McLennan et al. (2023) analyzes the mineralogical and geological characteristics of the reservoir based on drill cuttings and cores collected from 2018 to 2022. Figure 1 shows a geologic cross-section along the injection-production doublet's trajectory, highlighting well tracks, lithologies, and the reservoir's temperature gradient (Jones et al., 2024). The injection well 16A(78)-32 (blue) and production well 16B(78)-32 (red) are both deviated about 65° from vertical and run parallel, with the production well located roughly 100 meters above the injection well (Jones et al., 2024).

Preexisting fractures are essential for developing an Enhanced Geothermal System (EGS) reservoir, as they become permeable pathways for circulating fluid. These fractures can be identified in geophysical logs by increased sonic travel time and porosity, along with decreased density compared to surrounding rocks. Numerous studies have been conducted to characterize the FORGE site reservoir, focusing on the flow and transport of heat and mass in both preexisting and hydraulically fractured zones using geologic, geophysical, groundwater, physical, seismic, and geochemistry data (Jones et al., 2024; Moore et al., 2023; Podgorney et al., 2019; Podgorney et al., 2021; Simmons et al., 2016; Simmons et al., 2018; Wannamaker et al., 2020; Xing et al., 2024).

These fracture zones often contain high concentrations of secondary minerals formed by direct precipitation into open spaces, alteration of primary minerals, and fine-grained sheared rock. Unmineralized conductive fractures typically occur in localized clusters within the reservoir rock, with diverse orientations. Fracture zones also serve as sites for alteration and open-space filling mineralization. This paper aims to understand the mineralogical changes in the discrete fractured network (DFN) connected to well 16A during the circulation tests using reactive transport modeling.

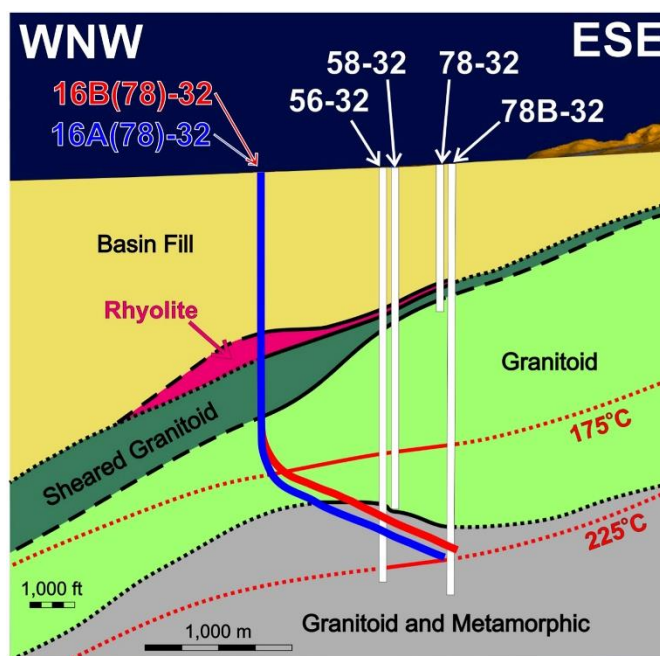


Figure 1: Geologic cross-section showing injection (16A) and production well (16B) doublet showing well tracks, lithologies, and the temperature gradient in the reservoir (Jones et al., 2024)

2. GEOLOGIC SETTING

The basement units at Utah FORGE are composed primarily of plutonic rocks, with deeper levels containing interleaved plutonic and metamorphic rocks. Above these basement units, the basin fill reaches a thickness of up to approximately 3000 meters and consists of a stratified sequence of geological units from the Tertiary, Quaternary, and Recent periods. As depth increases in this sequence, it includes alluvial fan deposits, lacustrine sediments with minor evaporites, and interbedded volcanic and volcanoclastic units of felsic to intermediate composition (Jones et al., 2024).

2.1 Mineralogy

Core samples from well 16A(78)-32 show weakly to moderately foliated granitoid with thin plagioclase and quartz dikes at the bottom (Jones et al., 2021). Strongly foliated, biotite-rich rock with quartz and plagioclase lenses, and folded dikes are found in specific intervals. Fractured zones exhibit distinctive mineralization, including early inclusion-rich albite ± quartz followed by Mg- and Fe-bearing carbonate in a fine-grained quartz ± illite matrix (Jones et al., 2021; Jones et al., 2024). This mineralization is sporadic throughout the well and other Utah FORGE wells. XRD analyses show secondary minerals, such as quartz, albite, carbonates, and clays, vary from less than 1% to over 90% by weight, with the highest concentration at the granitoid-orthogneiss contact. The Mineralogical composition considered in this study is based on bulk XRD results from well 16A(78)-32. Mineral abundances for depths of 9000-10000 feet are presented in Table 1 as weight percentages of the sample, with values rounded to the nearest whole number. Fields marked with "tr" (trace) indicate that the mineral is present but has an abundance of less than one weight percent as determined by Rietveld refinement. Furthermore, "tr" may also signify that the mineral was detected in the clay-sized fraction but not in the bulk sample, and/or that it was observed in low abundance during petrographic analyses.

Table 1: Mineralogical composition of well 16A(78)-32 at the FORGE site determined by bulk XRD analysis

Measured Depth (ft)	Quartz	Plagioclase	K-Feldspar	Biotite	Hornblende	Clinopyroxene	Titanite	Magnetite	Muscovite	Sillimanite	Epidote	Actinolite	Anhydrite	Calcite	Siderite	Illite	Chlorite
9000-9010	27	62	4	3	tr		1	tr								tr	tr
9100-9110	7	51	7	11	18	1	3		tr					1	tr	1	
9200-9210	40	33	17	4	1		2	tr	tr	tr						tr	1
9300-9310	11	52	27	5	1	1	tr	tr					tr	tr		1	tr
9400-9410	6	59	11	8	10	1	2	tr	tr					tr			tr
9500-9510	6	69	10	2	3		2	tr			4	tr		tr		2	tr

9600-9610	8	55	28	3	1		1	tr			tr			1		2	tr
9700-9710	36	42	8	3	1		tr	tr	tr		tr			tr		4	2
9800-9810	38	47	5	5	tr		tr	tr						tr		1	tr
9900-9910	14	50	5	8	10	1	3	tr	tr	tr	2	tr		1	tr	3	2
10000-10010	17	43	16	8	tr	3	1			1	1			tr		4	2

2.2 Water chemistry

The injected water is nearly fresh, as indicated by the sample taken from well 16A(78)-32 at 6:30 PM on July 19, 2023, which remained in the well. Table 2 shows sample data collected from well 16A(78)-32 at 6:30 PM on July 19, 2023, and from the producing well 16B(78)-32 at 3:00 PM on July 20, 2023.

Table 2: Aqueous species composition of well 16A(78)-32 and 16B(78)-32 at the FORGE site determined by chemical analysis

Species (mg/l)	16A(78)-32	16B(78)-32
Li	0.03	6.64
Na	41	0.22
K	3	81
Ca	24	7
Mg	5.46	109
B	0.18	3.48
SiO ₂	20	0.32
Cl	32	78
SO ₄	66	122
HCO ₃	78	115
F	0.74	276
As	0.01	0.37
pH	7.78	0.02

2.3 Numerical modeling

FALCON (Fracturing And Liquid CONvection) is a versatile subsurface simulator designed for addressing coupled thermal-hydraulic-mechanical-chemical (THMC) problems (Podgorney et al., 2019; Xia et al., 2017). It has been utilized in the study of geothermal reservoir dynamics, groundwater flow and transport, carbon sequestration, and more. Developed using Idaho National Laboratory's (INL) Multiphysics Object-Oriented Simulation Environment (MOOSE) framework (Gaston et al., 2012; Wilkins et al., 2021), FALCON features a modular, plug-and-play design. This architecture represents governing partial differential equations (PDEs) in a weak form, with the residual term described as a "kernel." These kernels are solved using a finite element scheme and can be coupled together for various applications. MOOSE's architecture allows for the convenient coupling of different processes. FALCON has been validated through several benchmark problems, and its source code is open source, with governing equations available in the MOOSE documentation.

The discrete fractured network (Figure 2) and reservoir model are derived from this data and a report on the large-scale upscaling of discrete fracture network modeling conducted for the Utah FORGE project in 2023 (Finnila, 2023). These models have been upscaled to a continuum mesh or grid with resolutions of 10 meters and 20 meters, providing reservoir properties such as fracture porosity, permeability, and compressibility. The DFN integrates data from surface fracture surveys and geophysical well logs to create planar fractures that function as a single hydrologic, mechanical, and chemical system. The reference DFN consists of two parts: 1) a deterministic set of fractures with known locations and orientations that intersect well 16(A)78-32, and 2) a stochastic set of fractures located away from well control. The orientations and intensity of the stochastic fractures are based on data from well 16(A)78-32, while fracture sizes are derived from nearby data collected in the Mineral Mountains. Multiple realizations can be generated to represent a range of possible natural fractures within the reservoir. For the THC simulations in this study, we used mineral kinetics data from Palandri and Kharaka (2004) and thermodynamic data from Wolery and Jove-Colon (2007)

3. RESULTS & DISCUSSION

The simulation results after a year of circulation tests, conducted in 10 stages with varying injection rates, are presented in Figures 2-12. Figures 2 and 3 illustrate the temperature changes in the fracture planes intersecting injection well 16(A)78-32 during the circulation operation. The equilibrium temperature in the annulus of the injection well and across the fracture plane is estimated to be 50°C, while the maximum production temperature is estimated to be 213°C.

The pH profile, shown in Figure 4, indicates a slightly acidic nature near well 16(A) within the DFNs. This pH change, primarily due to temperature variations, results in mineralogical changes. Figure 5 illustrates the dissolution of quartz and recrystallization slightly away from the injection well, a phenomenon also observed and reported by Jones et al. (2024). A similar profile, indicating retrograde precipitation of calcite, is shown in Figure 6. This occurred due to the movement of fluid further away from the injection well, where it encountered the hotter reservoir. The resulting temperature increase led to the precipitation of calcite during the operation.

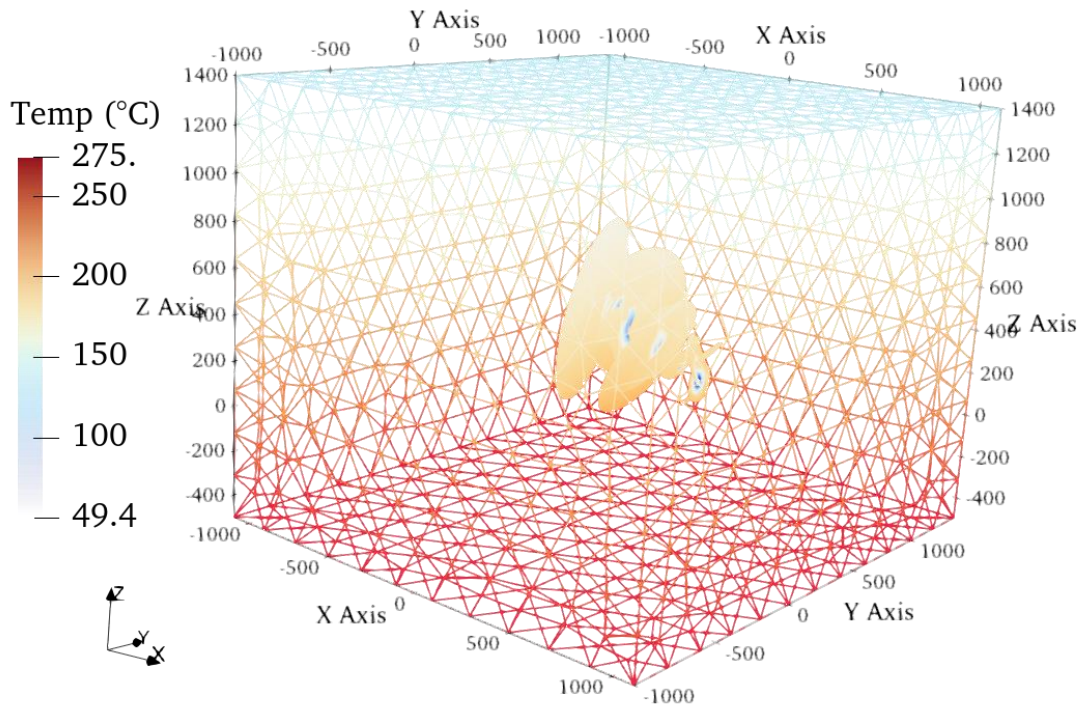


Figure 2: Temperature distribution in matrix and 2-D discrete fractured network after 1 year of circulation test.

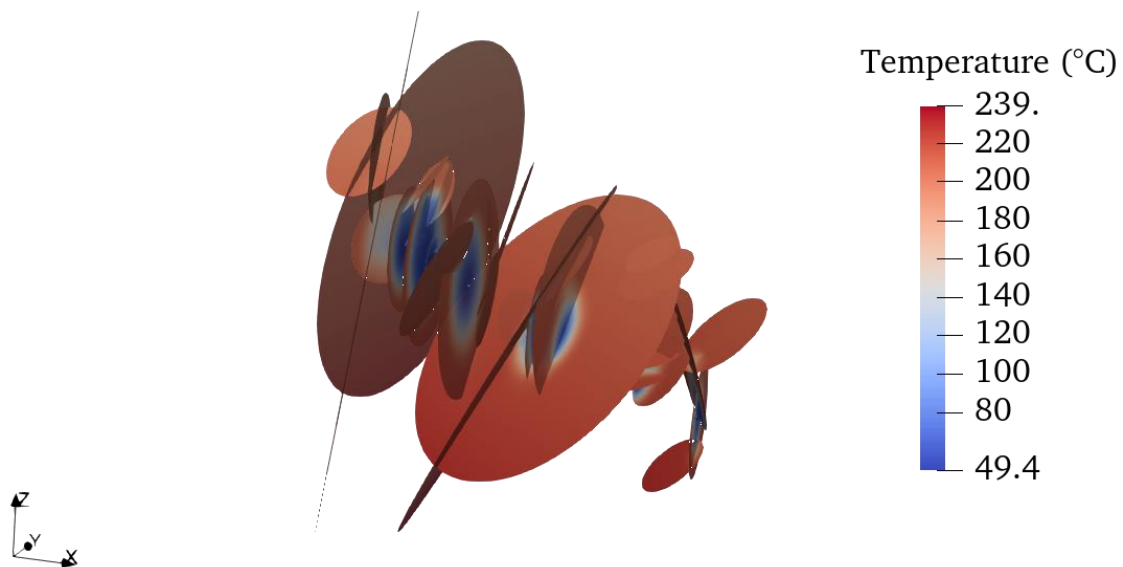


Figure 3: Temperature (°C) profile in the discrete fractured network after 1 year of circulation.

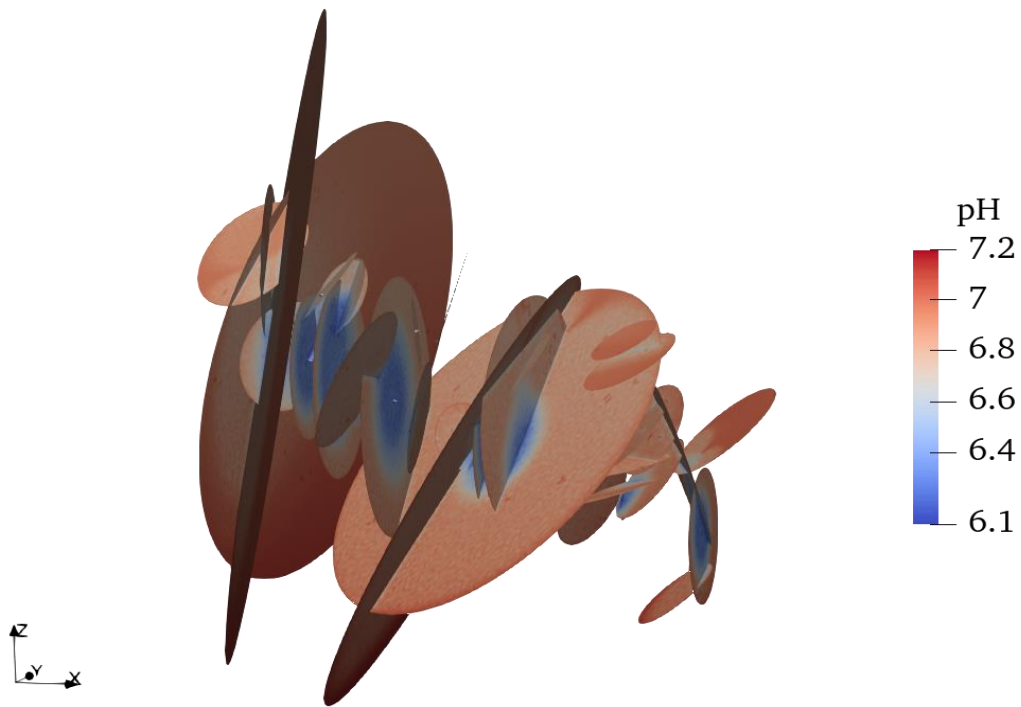


Figure 4: pH profile in DFN after 1 year of circulation test. The increased acidity shown in blue around the injection wells can be attributed to temperature-dependent changes in the activity of H^+ ions.

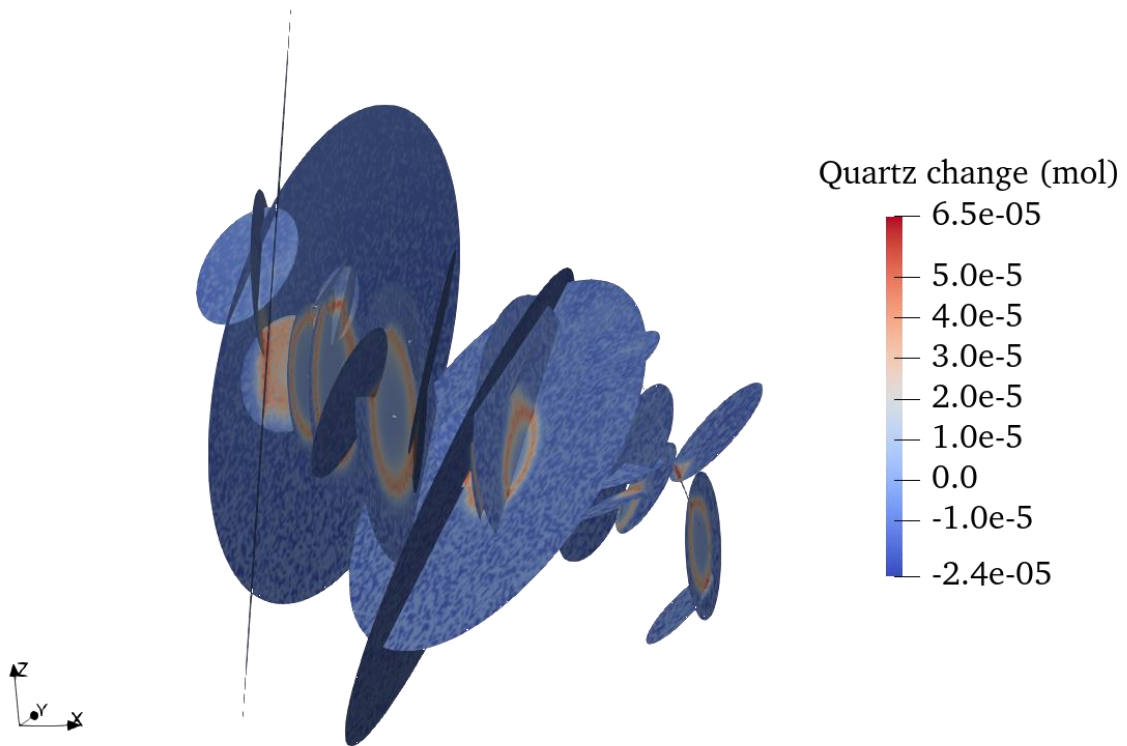


Figure 5: Changes in quartz (mol) in DFN after 1 year of circulation test. Quartz undergoes dissolution followed by recrystallization during temperature changes in the DFN as the plume travels further away from the well.

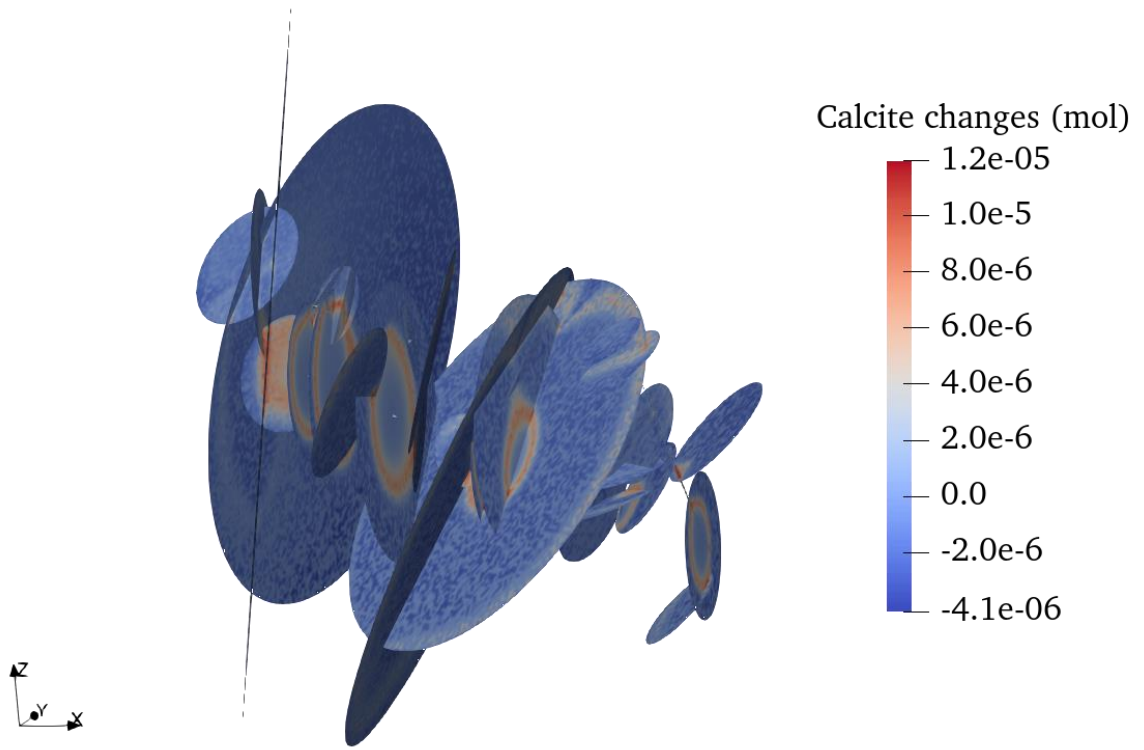


Figure 6: Changes in calcite (mol) in DFN after 1 year of circulation test. Calcite precipitation occurs as the temperature of the injected fluid rises while the plume moves further through the fractured network.

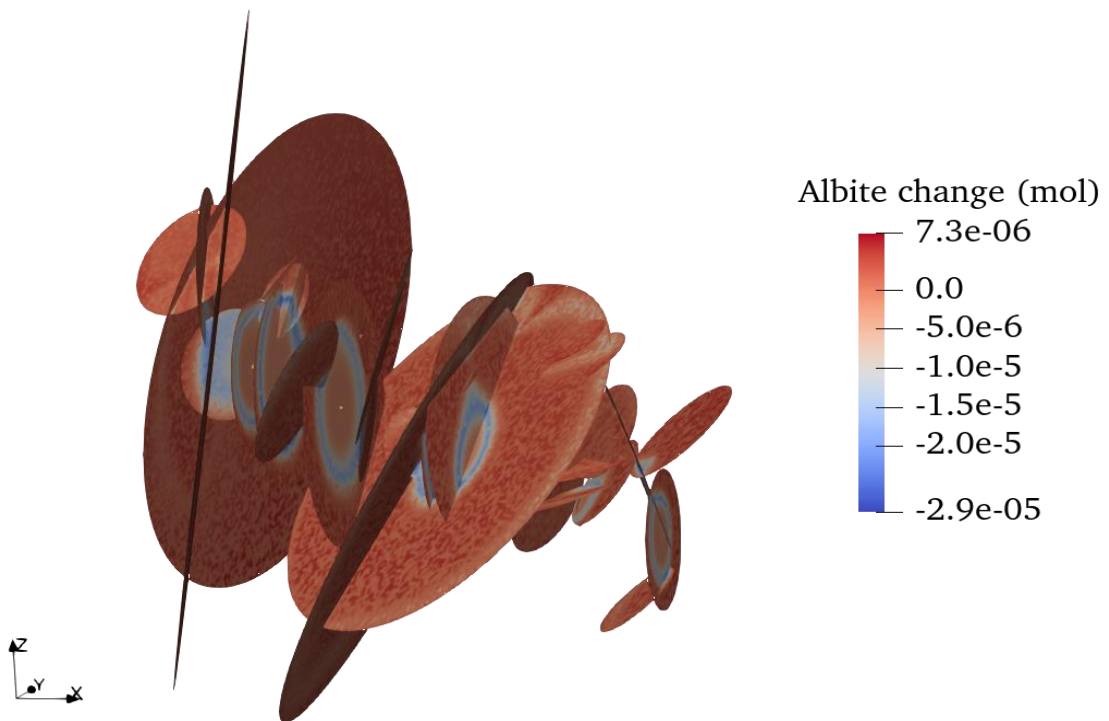


Figure 7: Changes in albite (mol) in DFN after 1 year of circulation test. Albite (plagioclase) dissolution is observed on the fracture planes slightly away from the injection wells.

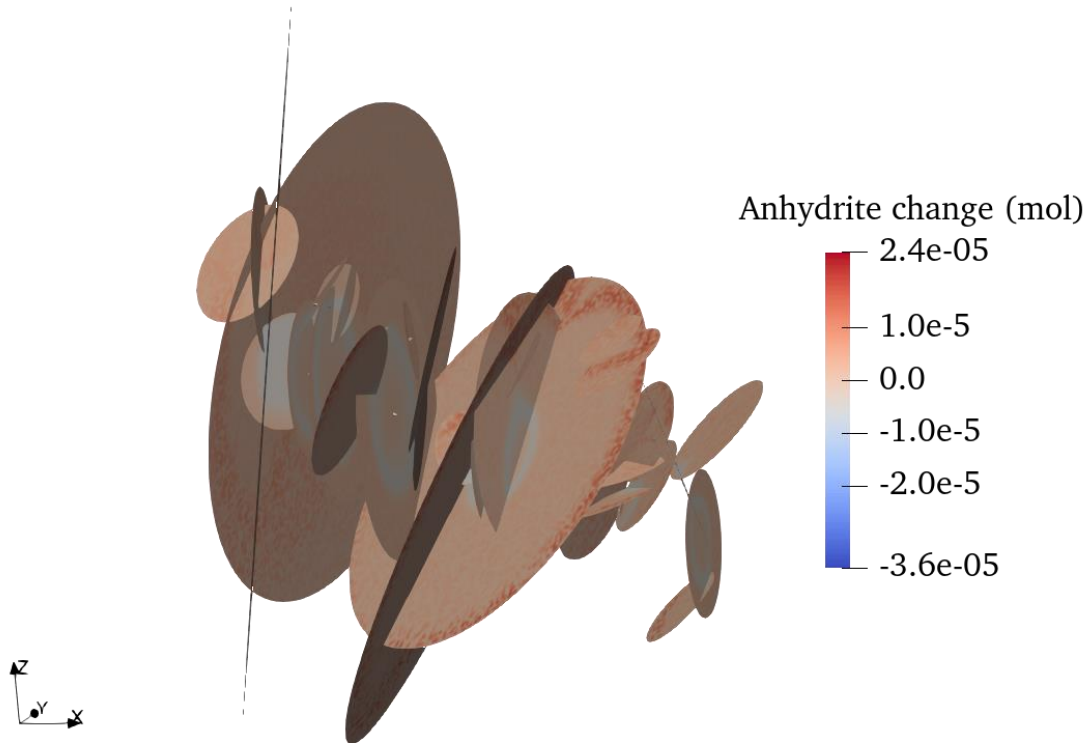


Figure 8: Changes in anhydrite (mol) in DFN after 1 year of circulation test. Anhydrite precipitation has been observed further away from the injection well. The pattern suggests dissolution followed by precipitation in the fractured planes.

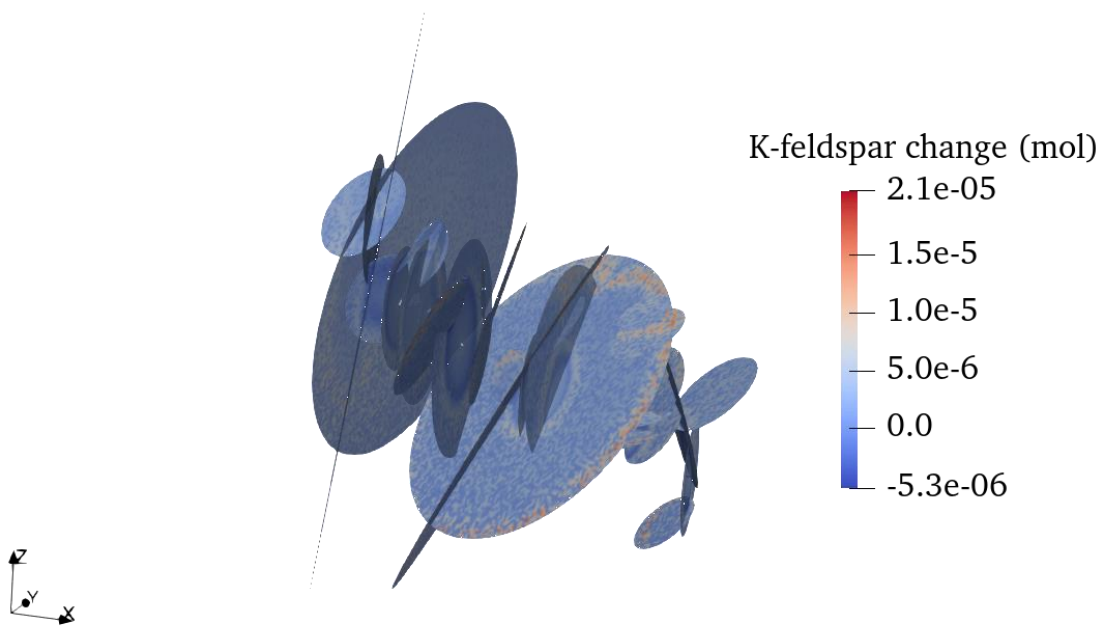


Figure 9: Changes in K-feldspar (mol) in DFN after 1 year of circulation test. Feldspar mainly dissolves, with a very narrow precipitation band forming in the outermost areas of the fractured networks.

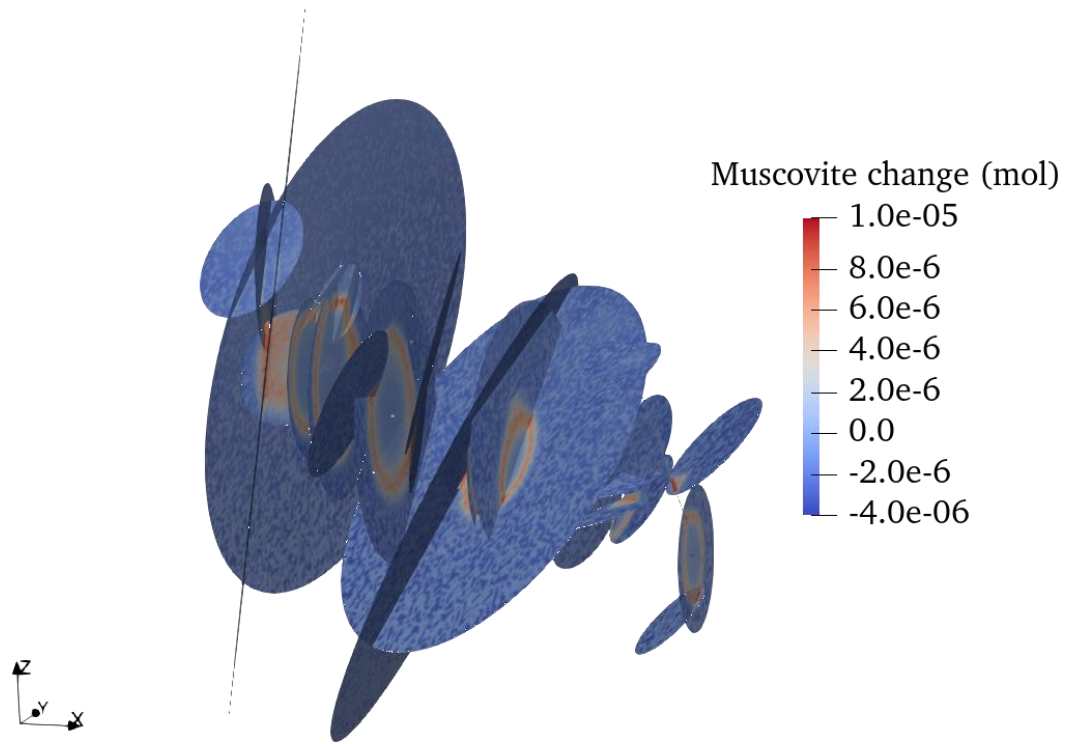


Figure 10: Changes in muscovite (mol) in DFN after 1 year of circulation test. The precipitation of muscovite exhibits similar characteristics to that of calcite, occurring near areas where the temperature begins to increase after injection into the fractured network.

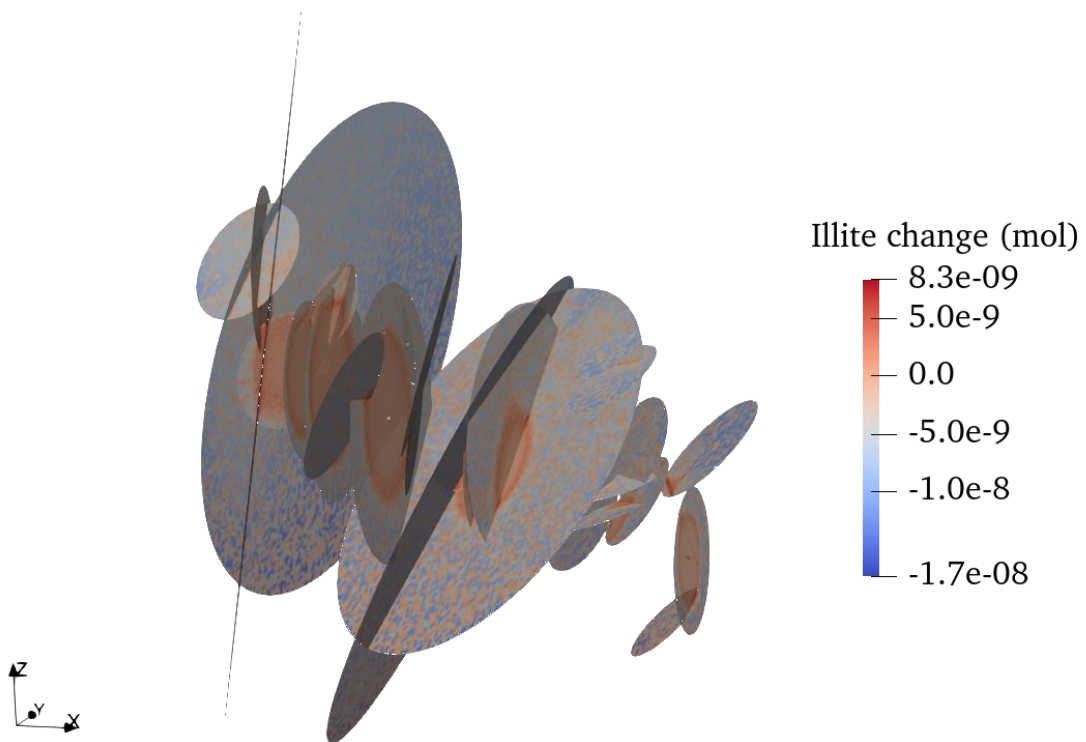


Figure 11: Changes in illite (mol) in DFN after 1 year of circulation test. Illite shows negligible dissolution except near the injection zone, where slight precipitation occurs due to temperature drop or cooling in that area.

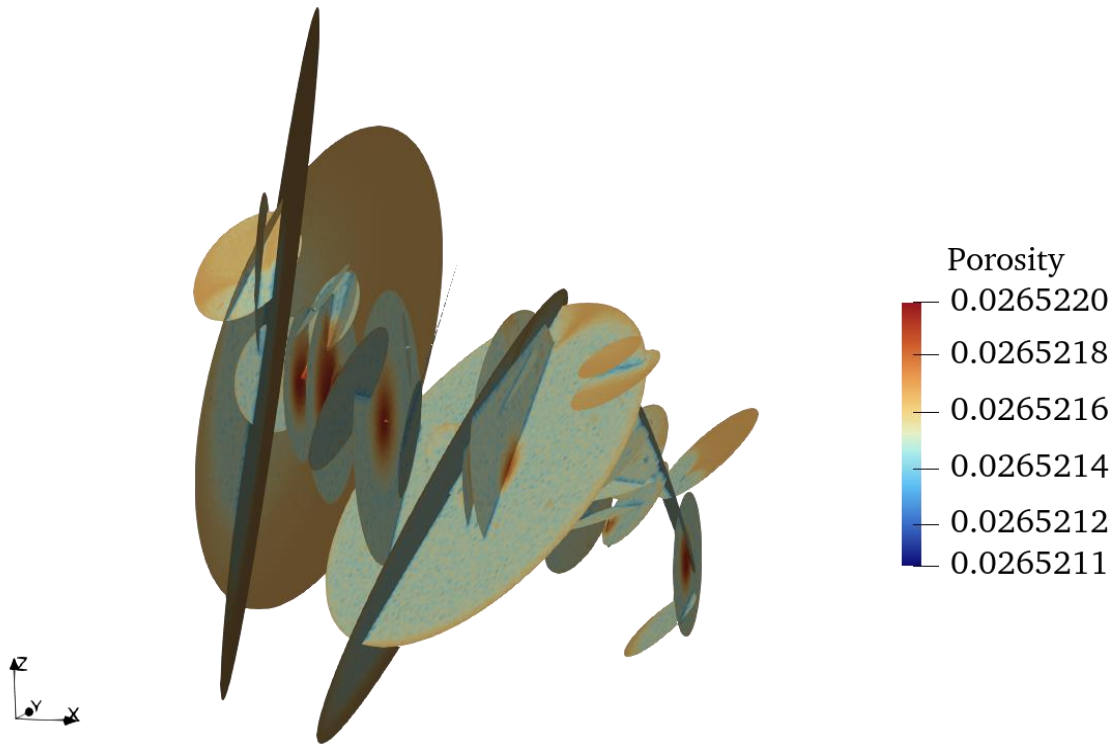


Figure 12: Porosity change profile in DFN after 1 year of circulation test. The initial porosity of the fractured network is 10%, and a ~2.6% increase is predicted during the circulation test experiments.

Albite shows dissolution in zones where calcite precipitates (Figure 7), while anhydrite (Figure 8) dissolves close to the well and precipitates further away. Muscovite (Figure 10) shows dissolution in most fractured planes, with precipitation occurring in a narrow band near the injection zone. Changes in feldspar, plotted in Figure 9, indicate dissolution with a few instances of precipitation in the outermost radial bands of the fracture planes. The net changes in porosity due to these mineralogical alterations result in a net gain of approximately 2.6%. This increase in porosity is also observed by (Jones et al., 2024). Temperature variations moving away from the injection zones lead to rapid solubility and recrystallization during phase-wise injections. These mineralogical changes occur rapidly due to the sharp temperature alterations in the injected fluid.

4. CONCLUSION & FUTURE WORK

Although there is significant consistency between the observed mineralogical changes (Jones et al., 2024) and the modeling predictions in this study, caution should be exercised when asserting the extent of these mineral alterations. The reaction kinetics could be further refined and validated with experimental/observed data, which can further alter both the magnitude and spatial distribution of these mineralogical changes within the fractured network, and consequently impacting the flow dynamics.

Furthermore, this study does not consider fracture heterogeneity, which can result in different levels of mineralogical alterations based on flow heterogeneity in fractures due to preferential flow in high-porosity areas. The accuracy in predicting flow paths and understanding the interaction between natural and engineered fractures remains uncertain, and current models do not precisely predict circulation loss. Another area of uncertainty includes the prediction of the distribution and geometry of fractured network, which can be improved with updated data from the next phase of tests at the FORGE site.

Additionally, using a 3-D fractured network instead of a 2-D model could lead to more accurate predictions of mineralogical and porosity changes, which are planned for future studies. Future THC (thermal-hydraulic-chemical) modeling will incorporate data from the upcoming phases of ongoing activities at the FORGE site to enhance the understanding of flow dynamics and related geochemical processes.

ACKNOWLEDGEMENTS

Funding for this work was provided by the U.S. DOE under grant DE-EE0007080 “Enhanced Geothermal System Concept Testing and Development at the Milford City, Utah FORGE Site”. We thank the many stakeholders who are supporting this project, including U.S. DOE Geothermal Technologies Office, Smithfield (Murphy Brown LLC), Utah School and Institutional Trust Lands Administration, and Beaver County as well as the Utah Governor’s Office of Energy Development.

REFERENCES

- Finnila, A. (2023). *Utah FORGE: 2023 Large Upscaled Discrete Fracture Network Models*. Retrieved from: <https://doi.org/10.15121/2007506>
- Gaston, D., Guo, L., Hansen, G., Huang, H., Johnson, R., Park, H., et al. (2012). Parallel Algorithms and Software for Nuclear, Energy, and Environmental Applications Part I: Multiphysics Algorithms. *Communications in Computational Physics*, 12(INL/JOU-10-20006).
- Jones, C., Moore, J., & Simmons, S. (2021). *X-ray diffraction and petrographic study of cuttings from Utah FORGE well 16A(78)-32*. Paper presented at the Transactions - Geothermal Resources Council. Conference paper retrieved from <https://www.scopus.com/inward/record.uri?eid=2-s2.0-85120041554&partnerID=40&md5=c61a2c3f955b72ad3e3141f92401ac22>
- Jones, C., Simmons, S., & Moore, J. (2024). Geology of the Utah Frontier Observatory for Research in Geothermal Energy (FORGE) Enhanced Geothermal System (EGS) Site. *Geothermics*, 122, 103054.
- McLennan, J., England, K., Rose, P., Moore, J., & Barker, B. (2023). *Stimulation of a High-Temperature Granitic Reservoir at the Utah FORGE Site*. Paper presented at the SPE Hydraulic Fracturing Technology Conference and Exhibition.
- Moore, J., McLennan, J., Allis, R., Pankow, K., Simmons, S., Podgorney, R., et al. (2019). *The Utah Frontier Observatory for Research in Geothermal Energy (FORGE): an international laboratory for enhanced geothermal system technology development*. Paper presented at the 44th Workshop on Geothermal Reservoir Engineering.
- Moore, J., McLennan, J., Pankow, K., Finnila, A., Dyer, B., Karvounis, D., et al. (2023). *Current Activities at the Utah Frontier Observatory for Research in Geothermal Energy (FORGE): A Laboratory for Characterizing, Creating and Sustaining Enhanced Geothermal Systems*. Paper presented at the 57th U.S. Rock Mechanics/Geomechanics Symposium.
- Palandri, J. L., & Kharaka, Y. K. (2004). *A compilation of rate parameters of water-mineral interaction kinetics for application to geochemical modeling*. Retrieved from
- Podgorney, R., Finnila, A., McLennan, J., Ghassemi, A., Huang, H., Forbes, B., & Elliott, J. (2019). *A framework for modeling and simulation of the Utah FORGE site*. Paper presented at the Proceedings of the 44th Workshop on Geothermal Reservoir Engineering, Stanford University, Stanford, CA, USA.
- Podgorney, R., Finnila, A., Simmons, S., & McLennan, J. (2021). A Reference Thermal-Hydrologic-Mechanical Native State Model of the Utah FORGE Enhanced Geothermal Site. *Energies*, 14(16), 4758. <https://www.mdpi.com/1996-1073/14/16/4758>
- Simmons, S., Kirby, S., Jones, C., Moore, J., Allis, R., Brandt, A., & Nash, G. (2016). *The geology, geochemistry, and geohydrology of the FORGE deep well site, Milford, Utah*. Paper presented at the 41st Workshop on Geothermal Reservoir Engineering.
- Simmons, S., Moore, J., Allis, R., Kirby, S., Jones, C., Bartley, J., et al. (2018). *A revised geoscientific model for FORGE Utah EGS Laboratory*. Paper presented at the Proc. of the 43rd Workshop on Geothermal Reservoir Engineering.
- Wannamaker, P. E., Simmons, S. F., Miller, J. J., Hardwick, C. L., Erickson, B. A., Bowman, S. D., et al. (2020). *Geophysical Activities over the Utah FORGE site at the outset of Project Phase 3*. Paper presented at the 45th Workshop on Geothermal Reservoir Engineering.
- Wilkins, A., Green, C. P., Harbour, L., & Podgorney, R. (2021). The MOOSE geochemistry module. *Journal of Open Source Software*, 6(68), 3314.
- Wolery, T., & Jove-Colon, C. (2007). *Qualification of thermodynamic data for geochemical modeling of mineral-water interactions in dilute systems*. Retrieved from
- Xia, Y., Podgorney, R., & Huang, H. (2017). Assessment of a Hybrid Continuous/Discontinuous Galerkin Finite Element Code for Geothermal Reservoir Simulations. *Rock Mechanics and Rock Engineering*, 50(3), 719-732. <https://doi.org/10.1007/s00603-016-0951-y>
- <https://link.springer.com/content/pdf/10.1007/s00603-016-0951-y.pdf>
- Xing, P., England, K., Moore, J., Podgorney, R., & McLennan, J. (2024). *Analysis of Circulation Tests and Well Connections at Utah FORGE*. Paper presented at the 49th Workshop on Geothermal Reservoir Engineering.